May 26-th, 1993
INFN PI/AE 93/12

L H B

A Fixed Target experiment at LHC to measure CP Violation in B mesons

Flavio COSTANTINI
University of PISA and INFN

Abstract

A fixed target experiment at LHC to measure CP violation in B mesons is presented. A description of the proposed apparatus is given together with its sensitivity on the CP violation asymmetry measurement for the two benchmark decay channels $B^\circ \to J/\Psi + K_S^0$, $B^\circ \to \pi^+\pi^-$. The possibility of obtaining an extracted LHC beam hinges on channeling in a bent silicon crystal. Recent results on beam extraction efficiencies measured at Cern SPS based on this technique are presented.

Invited talk at the: UNK B-FACTORY WORKSHOP
Liblice Castle (PRAGUE) Czech Republic Jan. 1993

May 26-th, 1993
INFN PI/AE 93/12

L H B

A Fixed Target experiment at LHC to measure CP Violation in B mesons

Flavio COSTANTINI
University of PISA and INFN

Abstract

A fixed target experiment at LHC to measure CP violation in B mesons is presented. A description of the proposed apparatus is given together with its sensitivity on the CP violation asymmetry measurement for the two benchmark decay channels $B^\circ \rightarrow J/\Psi + K^0_S$, $B^\circ \rightarrow \pi^+\pi^-$. The possibility of obtaining an extracted LHC beam hinges on channeling in a bent silicon crystal. Recent results on beam extraction efficiencies measured at Cern SPS based on this technique are presented.

Invited talk at the: UNK B-FACTORY WORKSHOP
Liblice Castle (PRAGUE) Czech Republic Jan. 1993

1 - INTRODUCTION

The possibility to use the next generation supercolliders (SSC, LHC) as hadronic Beauty Factories has been studied since 1984 at SSC Workshops [1], and several Expressions of Interest (EOI's) have been presented both for the SSC [2] and LHC [3].
It is now widely recognized that the measurement of the CP violation effect in the B system can be accomplished at the next generation supercolliders SSC and LHC with a sensitivity which is more than competitive with that achievable at the proposed e^+e^- asymmetric B-Factories.
This paper presents a Fixed Target experiment to measure CP violation in the B system based on the possibility of extracting the 8 TeV LHC proton beam using a bent silicon crystal [4]. A 10 % extraction efficiency of the LHC beam halo will give an extracted beam intensity of about 10^8 protons/sec allowing the production of as many as 10^{10} $B\bar{B}$ pairs per year, i.e. about two orders of magnitude more than what could be produced by an e^+e^- asymmetric B factory with 10^{34} $cm^{-2}s^{-1}$ luminosity [5] .
The physics motivations, extensively recalled elsewhere in this workshop, are quite briefly mentioned in Section 2. In Section 3 the first results obtained in 1992 by the crystal extraction tests are reported, followed by a possible extraction scheme for the LHC. The proposed detector is illustrated in Section 4, the achievable sensitivities on the benchmark decay channels $B^\circ \to J/\Psi + K^0_S$ and $B^\circ \to \pi^+\pi^-$ are discussed in Section 5 together with the elements affecting the final result of the asymmetry measurement.

2 - PHYSICS MOTIVATIONS : B mesons VERSUS K mesons

Present estimates of the CP violating asymmetry in Beauty decays based on the three quark generation Standard Model are larger than previously expected. In the $B^\circ \to J/\Psi + K^0_S$ decay a lower bound of $\sin(2\beta) = 0.55$ is predicted for a top quark mass of 140 GeV and for the f_b parameter in the range 200 MeV < f_b < 300 MeV [6].
This clearly indicates that the B mesons are a better choice than K mesons (where CP violating effects are $0(10^{-3}) \div 0(10^{-4})$) to verify if the Standard

Model predictions, based on the existence of a phase in the Cabibbo-Kobayashi-Maskawa matrix, are correct.

3 - BEAM EXTRACTION BY CRYSTAL CHANNELING

Channeling in a bent crystal appears as the most promising technique to produce an extracted LHC beam of intensity ~ 10^8 protons/sec in a fully parasitic mode, i.e. without interfering with the LHC operation as a 16 TeV collider. The crystal would be placed inside the beam pipe, at several σ 's from the beam center, intercepting only the beam halo which is naturally produced mostly by beam crossings in the interaction regions and by machine-lattice imperfections .
With a beam of $5 \cdot 10^{14}$ protons/ring circulating in the LHC, the expected halo is ~ $4 \cdot 10^9$ protons/s [7] . A bent Si Crystal with an extraction efficiency of 10 to 5 % will give an extracted beam of the intensity needed.
It is worth mentioning that the beam halo has to be removed anyhow by a dedicated 'cleaning section', as the quenching limit of Super Conducting LHC magnets is at about 10^7 protons/s .
Beam extraction by crystal channeling has already been achieved at accelerators with 8 GeV and 76 GeV beams [8] with efficiencies of $\cong 10^{-4}$, in 1984 and in 1989 respectively.
A larger extraction efficiency of 2 to 4 % has been measured in 1992 at the CERN SPS, extracting 120 GeV protons during the first year of the R&D program RD22 approved in 1991 [9], aimed at studying the LHC beam extraction.
The results of this measurement, although preliminary, are particularly relevant for the LHB approach. As they are not published yet [10], they are summarized in the following sections.

3.1 SPS BEAM EXTRACTION

A silicon monocrystal 3 cm long, 1 cm high and 1.5 mm thick was placed on a goniometer with an angular step of about 1 μradian. The goniometer was placed inside the SPS beam pipe on the same type of remote control mechanical support as a normal horizontal collimator. The crystal was

clamped on a cylindrical bender which bends the crystal {110} lattice planes by 8.5 mradian.
The extracted beam is detected by a telescope of scintillator counters which provide the trigger to the following detectors :

- a Cesium Iodide scintillating screen read by a CCD TV camera digitizing into 0.2 x 0.2 mm^2 pixels.

- two hodoscope planes 32 x 32 mm^2 which reconstruct horizontal and vertical beam profiles. Each plane consists of 32 scintillators 1 mm wide.

- a telescope of two pairs of Micro Strip Gas Chambers (MSGC) 25 x 25 mm^2 with 200 μm strip pitch. The two pairs are spaced 1 meter and each pair consists of a horizontal and a vertical plane. They are used to measure the horizontal and vertical directions of the extracted beam.

The evidence of beam extraction by crystal channeling was obtained using two different modes of SPS operation. First in the so-called "kick mode" and then in a "debunched mode", both at 120 GeV/c. A clear signal of extracted beam was seen in all the mentioned detectors for the two modes of operation, for the same angular position of the crystal. In Fig 1a the horizontal and vertical divergence of the extracted beam as measured by the MSGC is shown.
The "kick mode", not suited for collider operation, allows a fast crystal alignment, providing well-timed intense crystal illumination with large impact parameter. Positioning the crystal at 10 mm from the SPS equilibrium orbit, the expected impact parameter is about 100 μm.
In the "debunched mode" the horizontal beam emittance was continuosly blown-up by an electrostatic damper excited with white noise. A Monte Carlo simulation, reproducing the emittance blow-up rates, predicts impact parameter in the micron range, as expected at LHC.The intensity of the extracted beam could be controlled by the strength of the white noise damper excitation.
Two bent silicon crystal were tested, giving preliminary extraction efficiencies between 2 and 4% as shown in Table 1 , where it is relevant to

remark that the presence of the crystal was not affecting the beam lifetime more than a normal collimator.
The extraction tests will continue in 1993 to measure in particular the channeling angular acceptance, the divergence of the extracted beam, the relative contribution of single pass versus multiple pass extraction efficiency.

Sample	Crystal 1	Crystal 1	Crystal 2	Crystal 2
Beam lifetime	34h00	14h30	75h00	16h30
Protons on Crystal (Hz)	$6.9\ 10^6$	$16.\ 10^6$	$3.7\ 10^6$	$20.\ 10^6$
Mean Impact Parameter (μm)	0.1	0.6	< 0.1	0.4
Signal Rate (Hz)	$.29\ 10^6$	$.75\ 10^6$	$.90\ 10^6$	$.60\ 10^6$
Background Rate (Hz)	$.07\ 10^6$	$.16\ 10^6$	$.25\ 10^6$	$.20\ 10^6$
Extraction Efficiency (%)	≥ 3.2	≥ 3.7	≥ 1.8	≥ 2.0

TABLE 1 : Extraction efficiencies

3.2 SPS BEAM BENDING

The RD22 program aims also at measuring the beam-bending efficiency by crystal channeling as a complementary aspect of the beam extraction efficiency. In the bending case the beam illuminates the whole entrance face of the crystal and the channeling properties are mostly due to the channeling in the bulk of the crystal.
In the extraction case the beam illuminates the crystal entry face with an impact parameter at a micron level only. The extraction is then essentially sensitive to the surface channeling properties of the crystal face tangent to the circulating beam halo.
As a consequence the extraction efficiency is affected by mostly two factors:

- the degree of parallelism of the external face of the crystal with respect to the lattice plane, indicated as miscut angle; present techniques keep this factor under control reaching miscut angles below about 25 μradian [11] .

- the various mechanical and chemical processes used to obtain the crystal face tangent to the beam halo, as cutting, polishing, chemical etching.

In order to measure also the bending efficiency of a given crystal, besides the extraction efficiency , a testing set-up has been prepared at the CERN H8 micro-beam line. This beam line has the property of providing a 450 GeV/c proton beam with a horizontal divergence of few μradian, i.e. quite smaller than the planar critical angle ψ_P = 14 μradian at this momentum value. Unfortunately a faulty magnet has caused an order of magnitude increase in the horizontal beam divergence during 1992 H8 measurements.

The bending efficiencies were measured for three values of the crystal bending angle: 8.5, 5.7, 3.0 mradian . The same crystal was used by varying the angle of the mechanical bender. Fig. 1b shows the three overlapped and normalized distributions of the bent beams.The corresponding peak bending efficiencies are listed in the first line of table 2 . In the second line are listed the efficiencies corrected [12] by deconvoluting the measured beam divergence, to take into account the effect of the beam divergence due to the faulty magnet .

Due to access difficulties during SPS operation, the crystal used to measure the bending efficiencies in 1992 could not be one of the two crystals used for the extraction measurements.

The quite encouraging results obtained so far by the RD22 program at the CERN SPS, indicate that the value of crystal extraction efficiency needed for the proposed LHB experiment is already within reach.

Bending angle (mradian)	3.0	5.7	8.5
Peak deflection efficiency (%)	20 ± 2	10 ± 1	7.7 ± 0.3
Computed deflection efficiency in ± ψ_P range (%)	54 ± 2	33 ± 5	16 ± 3

TABLE 2. Bending efficiencies of 450 GeV/C protons for three crystal bending angles. The first line shows the peak efficiencies; the second line shows the efficiencies evaluated taking into account the crystal acceptance in ± ψ_P the planar critical angle. The quoted errors are statistical only.

3.3 LHC BEAM EXTRACTION SCHEMES.

Two possible schemes for the LHC beam halo extraction based on crystal channeling have been preliminarly considered.
A first scheme considers the possibility of extraction in the horizontal plane in one of the four odd LHC interaction regions, taking advantage of the outward crossing of the beams to avoid interference between the main tunnel and the extraction tunnel. The magnetic optics scheme considered is similar to the one proposed for the beam dumping section ; here the bent crystal replaces a fast kicker bending circulating protons exactly by the same amount . This possibility has already been presented at the Aachen LHC meeting [13] .
A second scheme considering the possibility of beam extraction in the vertical plane has been worked out more recently [14] . The magnetic optics scheme of the vertical extraction is similar to the one proposed for the beam injection from the SPS into LHC, with the addition of a warm septum magnet (see Fig. 2) .
In both the horizontal and vertical extraction schemes a 3 to 5 cm long silicon crystal bends the LHC 8 TeV protons by 0.7 mradian; additional bending is given downstream by either a dipole or a quadrupole, respectively, of the normal LHC lattice. The final bending required to clear the LHC tunnel is given by a string of 5 Super Conducting (S.C.) dipoles, each with a bending strength similar to that of LHC S.C. dipoles.
It might be interesting to note here that the bending power of the 5 cm long bent crystal is one fourth that of a normal LHC S.C. dipole, which has a 10 T field extending over 10 m.

3.4 RADIATION DAMAGE

From the point of view of the radiation damage of the crystal exposed to the LHC beam halo, the results are encouraging. The channeling properties are first of all less affected than the electrical properties of silicon exposed to radiation damage: channeling of high energy protons in fact could be affected essentially by dislocations in the crystal structure.

The channeling properties of a silicon crystal have been measured after an exposure up to 10^{18} protons/cm^2 and found unchanged [15]. Shortly, the channeling properties of a crystal exposed to beam fluencies up to about 10^{20} protons/cm^2 will be measured [16]. This exposure corresponds to about one year of operation of a crystal on which protons impinge with a 1 μm impact parameter.

It has to be mentioned that, as the crystal is mounted on a goniometer with a step size of 1 micron and controlled by a laser based alignment system, it is possible to move it vertically, changing the impact area of the circulating halo in case of a local damage.

4 - THE LHB EXPERIMENTAL APPARATUS

The LHB experimental apparatus is a large acceptance (2 - 75 mradian) and powerful spectrometer on a dedicated beam line.

This choice is based on the consideration that only this approach gives the possibility of optimizing the performances of all the various detectors needed. We believe that an optimization without compromises is necessary to obtain the most precise CP violation measurements achievable at a fixed target experiment.

Different approaches based on gas jet targets or internal wire targets [17] are necessarily based on compromises dictated by the constraints of developing the experimental apparatus both inside the beam pipe (e.g. vertex detectors in Roman pots) and around it (or them, as in the LHC case). This will lead inevitably to face limitations due to the presence of vacuum pumps, machine magnets and problems due to beam pipe heating for degassing, etc.

An example of such compromises is the need to place silicon vertex detectors inside Roman pots as close as possible to the full LHC circulating beam to maximize the acceptance and the opposite need of reducing the danger of the radiation exposure .

Only a brief description of the apparatus shown in Fig. 3 is given here. The collaboration is presently preparing a first detailed design which will be described in a Letter of Intent. This document will be presented to the CERN LHC Commettee in a few months.

4.1 - THE TARGET

A 5 % λ_I Cu target hit by the extracted beam of about $2 \cdot 10^8$ protons/s will give a maximum of about 10 MHz of interaction rate. Following the approach of the WA92 experiment [18], a threshold on the pulse heigth of a silicon microstrip counter placed on the downstream face of the target, ensures that an interaction has occurred inside the target.
The transverse position of the primary vertex is determined by a telescope of microstrip chambers placed upstream of the target. This information is used by a trigger hardware processor to compute the impact parameter of tracks seen in the decay detector, described in the following section.

4.2 - THE MICRO-VERTEX DETECTOR.

The micro vertex detector is placed immediately after the target. It consists of two parts: a decay detector first, followed by a vertex detector (see Fig. 4). The decay detector consists of 20 planes of 10 μm pitch silicon microstrips for a total of about 80.000 channels. The thickness of each plane is 200 μm giving ≤ 0.9 % λ_I overall and the plane spacing is 5 mm, thus extending the decay detector over 10 cm. The pulse height read-out will reject fake secondary vertices due to reinteractions in the silicon planes.
The vertex detector consists of 20 planes of 25 μm pitch silicon microstrips, with about the same number of channels as the decay detector. The vertex detector is sandwiched by 6 planes of silicon pixels to solve track ambiguities, bringing the total number of electronic channels to about 1.2 10^6. These channels will be equipped with 20 ns electronics [19].
The 10 cm distance spanned by the decay detector allows an almost 'visual' observation of B decays over several decay lengths. It is expected in fact to perform the measurement of the decay vertices with a longitudinal precision of about 0.5 mm and a transverse precision at the micron level.
These achievable precisions are more than adequate to measure both the B impact parameter ($c\tau_B \cong 390$ μm) and the typical B decay length of about 3 cm and to measure B_s° oscillations given by $x_s \geq 12$
We believe that the full extension of the micro vertex detector is one element of the strength of the LHB approach, together with the possibility of

exploiting this detector at the trigger level. The WA92 experience has already shown that, by using the decay detector information, the Beauty Contiguity Processor (BCP) is capable of providing a reasonably fast trigger with an adequate enrichment factor [18] .

4.3 THE TWO DIPOLE MAGNET SCHEME

The momentum of charged particles is measured by two dipoles with opposite field but equal $\left| \int \vec{B} \cdot \vec{dl} \right|$. Each dipole provides a transverse momentum kick of 2.1 GeV/c . An advantage of such a scheme is that charged particles produced in the target at a given angle with respect to the beam direction exit from the second magnet conserving their initial production angle.

This property, exploited at the trigger level (see later) for muons, has also the advantage that the detectors following the second magnet are more compact in the direction of the bending plane than they would be in a single dipole scheme with the same total $\left| \int \vec{B} \cdot \vec{dl} \right|$.

4.4 THE RICH DETECTOR.

A RICH detector up to 10 m length can be accomodated between the two dipoles to give π/k separation up to 300 GeV/c [20]. This separation is essential for the identification of the decay channel $B^\circ \rightarrow \pi^+\pi^-$ from the physics background given by other non-CP-violating decay channels, as detailed in section 5.2 .

4.5 THE ELECTROMAGNETIC CALORIMETER

The electromagnetic calorimeter could be of the "tile" type in which scintillator and lead tiles of different thickness are assembled in towers. Light collection is achieved by wavelength-shifting longitudinal fibers uniformly sparse in the body of the towers. This technique has the advantage

of offering, at moderate cost, good spatial granularity, excellent hermeticity due to minimal dead space between towers and good energy resolution.
The performances of a prototype calorimeter have been already measured on a test beam [21]. A resolution $\sigma/E = 10\%/\sqrt{E}$ and a π/e rejection of 10^{-3} have been measured and seem adequate.
A tracking preshower in front of the calorimeter will distinguish electrons from neutrals at the trigger level .

4.6 THE MUON SECTION.

After the e.m. calorimeter the muon section, consisting of two iron filters of 3 m length each interleaved with tracking chambers, completes the spectrometer.The 6 meters of iron corresponding to a muon momentum cut of 10 GeV are found to be adequate to considerably reduce the background while giving a negligible signal loss. The chamber spatial resolution needed to provide the desired momentum resolution, is estimated to be of the order of 100 μm .

4.7 THE TRIGGER.

The trigger will be based on a multi-level architecture with the possibility of adding specialized triggers for particular decay channels (e.g. $B^\circ \rightarrow J/\Psi + K^0_S$, $B^\circ \rightarrow \pi^+\pi^-$). The muon trigger is extensively illustrated in a separate contribution to this workshop [22] and it is here only briefly mentioned.
The muon P_T trigger is based on the property of the two dipole magnet scheme of letting charged particles exit the second dipole with their initial production angle.
The relation $P_{TB} = K\,\theta\,/d$ can be established, where θ is the production angle , d is the displacement, P_{TB} is the P_T in the bending plane due to the first dipole and K is a constant proportional to $B\cdot L$. The θ measurement can be performed at the trigger level using the information from the muon chamber placed after the iron filter, allowing the computation of d and hence of the muon P_{TB} . Finally the P_T of the muon can be obtained using also the muon chamber information on the non-bending plane.

The initial 10^7 Hz interaction rate drops to about $2 \cdot 10^4$ Hz with the requirements on the muon range and a muon P_T cut of 1 GeV/c.
A further reduction to about 2 kHz will be obtained by a P_T cut of 1 GeV on 1 hadron (or more) , which could be obtained using a set of butterfly type hodoscopes or chambers following the scheme of the Omega experiment.
At about 2 kHz rate an Impact Parameter trigger, based on the fast (< 10μs) Beauty Contiguity Processor similar to the model developed for the WA92 experiment [23], could bring the rate to about 500 Hz .
An electron trigger based on the high granularity of the electromagnetic calorimeter possibly matched to the preshower information is under study.
The study requires a detailed GEANT simulation of the apparatus to evaluate correctly the conversion of all neutrals generated in Monte Carlo events.
The importance of an electron trigger is quite relevant as it gives a factor four increase in the collected statistics for the $B^\circ \rightarrow J/\Psi + K^0_S$ decay channel and a factor two for $B^\circ \rightarrow \pi^+\pi^-$.

5 - THE LHB EXPERIMENTAL PROGRAM

The collection of 10^{10} $B\overline{B}$ pairs in one or two years gives access to an experimental program covering from CP violation to precision B studies.
The precise measurement of CP asymmetries in various B decay channels overconstrains the values of the angles in the so called unitary triangle.
The simultaneous measurement of these angles, which are related to the coefficients of the Cabibbo-Kobayashi-Maskawa matrix, is a stringent test of the CP violation predictions in the framework of the Standard Model.
In addition, the capabilities of the proposed apparatus allow the exploitation of the large B sample collected, to perform precision studies of B lifetimes, B^0_S oscillations, rare decays, B_C and B-Baryons.

5.1 THE BENCHMARK DECAY CHANNEL $B^\circ \rightarrow J/\Psi + K^0_S$.

The simulation results on this decay channel, called 'gold plated' for its eccellent signature and often used as term of reference for experiment comparison purposes , have been obtained using PYTHIA [24] and an angular acceptance of the LHB apparatus between 2 and 75 mradian [25] .

The momenta of charged particles were smeared to simulate a spectrometer resolution of $\Delta P/P = 10^{-4}$ P (GeV/c) .

Resonant background.

Requiring at least a muon and a hadron, both with $P_T \geq 1$ GeV/c, the invariant mass distribution shown in Fig. 5b is obtained if a cut of P_T (pair) ≥ 0.8 GeV/c is applied to the pair of hadrons used to reconstruct the K^0_S . No hadron identification and no vertex constraint is assumed for the pair of hadrons.

The B° invariant mass is obtained by a mass constrained fit of J/Ψ and K°. In the same plot the contamination of the decay channel $B^\circ \to J/\Psi + K^0_S + \pi^0$ to the gold plated one is shown. Even assuming a 10 times bigger branching ratio (B.R.) for this physical background, the signal contamination is small. Applying a vertex association cut for the two hadrons used in the computation of the K° invariant mass, this contamination will be reduced to a completely negligible level.

Another contribution to the elimination of this physics background could come, already at the combinatorial level, from the hadron identification given by the RICH.

Non-resonant background.

The following sources of non resonant combinatorial background have been considered:

- "strong" J/Ψ production + K°
- inclusive $B^\circ \to J/\Psi + X + K^\circ$

A B.R. of $2\cdot10^{-5}$ was assumed for the decay $B^\circ \to J/\Psi + K^0_S \to \mu^+\mu^- + \pi^+\pi^-$.

The B° decay vertex position is reconstructed from the vertex of the lepton pair forming the J/Ψ mass.

In addition to the procedure and cuts already mentioned for the resonant background rejection it is required that the distance of the J/Ψ vertex from the primary vertex is ≥ 10 mm. This cut rejects the prompt J/Ψ production which is the dominant background component. The results are shown in Fig 5a .

The measured ISR value at $\sqrt{s}$ = 63 GeV [26] of the process pp $\rightarrow$ J/Ψ + X has been scaled up by a factor 1.5 to $\sqrt{s}$ = 123 GeV. The scaling factor has been obtained using the universal scaling function P ($M_V / \sqrt{s}$) mentioned in the quoted reference, where M_V is the mass of the vector meson produced.

5.2 THE BENCHMARK DECAY CHANNEL $B^\circ \rightarrow \pi^+\pi^-$

A detailed simulation study has been carried on this benchmark B° decay, including multiple scattering effects in the decay detector, assuming an average traversal of 10 Si planes [27].
Inside the geometrical acceptance previously defined, the following cuts were applied to reduce the combinatorial background:

- for the Z_B coordinate of the B decay vertex (i.e. along the beam direction) measured from the center of a 5 mm thick target, 10 mm < Z_B < 90 mm.

- for the closest distance d of any other track to the B decay vertex, $d > 10$ μm .

- for the B momentum P_B in order to improve B mass resolution, $P_B < 600$ GeV/c.

- for the P_T of hadrons, $P_T > 1$ GeV/c.

With these cuts the acceptance for the $B^\circ \rightarrow \pi^+\pi^-$ signal is 25%.

<u>Background from other B° decays.</u>

Non resonant background from 3-body decay $B^\circ \rightarrow \pi^+\pi^-\pi^\circ$ contributes to the signal region in fig. 6a where a
B.R. ($B^\circ \rightarrow \pi^+\pi^-\pi^\circ$) / B.R. ($B^\circ \rightarrow \pi^+\pi^-$) = 4 was assumed. A more serious background contribution comes from $B^\circ \rightarrow \rho^\pm\pi^\pm$ as shown in fig. 6b where again a factor 4 in the B.R. of background with respect to signal was assumed.

A conservative production ratio of $\rho\pi : \pi\pi \cong 8$ gives a signal to background ratio of better than 6 : 1 which could be improved significantly by an increase of momentum resolution up to $\Delta p/p = 0.5 \cdot 10^{-4}$ p .
The most important background contribution comes from the penguin decay $B^{\circ} \to K^{+}\pi^{-}$ ($\overline{B^{o}} \to K^{-}\pi^{+}$), whose B.R. is predicted to be of the same order of the signal. Fig. 6c shows that the invariant mass distribution overlaps considerably with the signal, making particle identification (e.g. by a RICH counter) essential for the CP violation measurement in the $\pi^{+}\pi^{-}$ channel.
In order to reduce the $K\pi$ background contribution both from B° and B_{S} decays, a K/π separation in a wide momentum range is needed. This is shown in Table 3 where the fraction of $B^{\circ} \to \pi^{+}\pi^{-}$ decays is given for minimum and maximum pion momentum cuts.

Min. Cut P_{π} (GeV/c) >	30.	40.	50.	100.
Fraction (%) of $B^{\circ} \to \pi^{+}\pi^{-}$	92.	84.	76.	40.
Max. Cut P_{π} (GeV/c) <	300.	350.	400.	450.
Fraction (%) of $B^{\circ} \to \pi^{+}\pi^{-}$	68.	80.	89.	95.

Table 3. Fraction of events for minimum/maximum p_{π} cuts (for $p_{B} < 600$ GeV/c).

5.3 ASYMMETRY MEASUREMENT

There are several physics and experimental factors affecting the asymmetry measurement, as for instance tagging, intrinsic production asymmetry and lepton misidentification.
The contributions of all these factors has been evaluated for the LHB detector [28] and are briefly summarized here, assuming the $B^\circ \rightarrow J/\Psi + K_S^0$ decay as an example.

TAGGING

For the cases in which the final CP eigenstates F and $\overline{F}$ are such that $F = \overline{F}$, the only way to tell the initial flavour of the decaying B° meson is to "tag" the initial flavour of the partner b hadron, e.g. measuring the lepton sign in its semileptonic decay.
The measured asymmetry in the case of the following final states :

$$b \rightarrow \overline{B^0} \rightarrow J/\Psi + K_S^0 \quad , \quad \overline{b} \rightarrow l^+ x$$

$$\overline{b} \rightarrow B^\circ \rightarrow J/\Psi + K_S^0 \quad , \quad b \rightarrow l^- x$$

where l indicates a lepton, would then be

$$A\,(t) = \frac{N\,(B^\circ \rightarrow J/\Psi + K_S^0\,) - N\,(\overline{B^0} \rightarrow J/\Psi + K_S^0\,)}{N\,(B^\circ \rightarrow J/\Psi + K_S^0\,) + N\,(\overline{B^0} \rightarrow J/\Psi + K_S^0\,)} =$$

$$= \frac{N\,(\,J/\Psi \;\; K_S^0 \;\; l^-\,) - N\,(\,J/\Psi \;\; K_S^0 \;\; l^+\,)}{N\,(\,J/\Psi \;\; K_S^0 \;\; l^-\,) + N\,(\,J/\Psi \;\; K_S^0 \;\; l^+\,)}$$

When evaluating A(t), several effects have to be considered :

1) The probability that the b-tagging hadron can oscillate into its anti-particle has to be taken into account.

$$\chi = \frac{N(b \to l^-)}{N(b \to l)} = f_0 \chi_0 + f_s \chi_s$$

$$\bar{\chi} = \frac{N(\bar{b} \to l^+)}{N(\bar{b} \to l)} = \bar{f}_0 \chi_0 + \bar{f}_s \chi_s$$

where χ ($\bar{\chi}$) is the average probability for $\bar{b} \to b$ ($b \to \bar{b}$) through mixing,

$$\chi_0 = \frac{N(\text{ B decays as } \bar{B})}{N(\text{ all B })}$$

is the mixing probability measured by ARGUS and CLEO, and f_0 ($\bar{f}_0$), f_s ($\bar{f}_s$) are the fragmentation probabilities of B° ($\bar{B}^o$) and B_S ($\bar{B}_s$) respectively.

2) B° and $\bar{B}^o$ are not produced in exactly equal amounts from a pp initial state due to different recombination probability of b, $\bar{b}$ with the four u-quarks and two d-quarks present in the initial state.

It has to be recalled that the ratios $\bar{f}_0/f_0$ and $(\bar{f}_0 - f_0) / (\bar{f}_0 + f_0)$ can be derived from experimental data using the easily reconstructed channel $B^\circ \to D^{*-}\pi^+$.

3) The detected lepton can be produced by the semileptonic charm decay in the $b \to c$ cascade, thus giving a wrong tagging lepton sign.

4) The lepton can be faked by a π or a K. Indicating the absolute multiplicities m_+ and m_- for faked positive and negative tag leptons:

$$m_+ = N(\pi^+) \bullet \delta_\pi \bullet \eta_{\pi^+} + N(K^+) \bullet \delta_K \bullet \eta_{K^+}$$
$$m_- = N(\pi^-) \bullet \delta_\pi \bullet \eta_{\pi^-} + N(K^-) \bullet \delta_K \bullet \eta_{K^-}$$

where η_X is the kinematical tagging acceptance, δ_X is the misidentification probability for hadron X and N(X) is the average number of hadrons X in the event.

The expected misidentification probabilities are $\delta_K \approx 2\%$ and $\delta_\pi \approx 1\%$. These values are a sum of the μ and e misidentification probability: more precise estimates require a full detector simulation which is presently under way.

The measured asymmetry A_{obs} can be expressed as :

$$A_{obs} = I + K \bullet A$$

where A = A (t) is the asymmetry previously defined, I is the "intrinsic" global asymmetry and K is a "dilution factor".

In fig. 7 the measured asymmetry A_{obs} is shown versus the physical asymmetry A, with the set of parameter values specified in the following, obtaining I = - 0.003 and K = 0.45 . A P_T cut of 1 GeV/c has been applied on the tag lepton, using $f_0 = 0.404$, $\overline{f_0} = 0.410$, $f_s = 0.091$, $\overline{f_s} = 0.119$, N (K^-) = 1.12, N (π^-) = 8.1, N (π^+) = 9.3 .

In table 4 the LHB sensitivities for the decay channels examined in detail in sections 5.1 and 5.2 are indicated, showing the estimated contribution of the various factors affecting the final results. The final rows show the dilution factor, the mistagging factor and the reduction due to the time fit of the B° oscillations assuming $x_d = 0.68$ [29].

DECAY CHANNEL	$B^\circ \to J/\Psi + K^0_S$		$B^\circ \to \pi^+\pi^-$	
$B\overline{B}$ Pairs		$2 \cdot 10^{10}$		$2 \cdot 10^{10}$
Hadronization to $B^\circ/\overline{B^\circ}$	0.8	$1.6 \cdot 10^{10}$	0.8	$1.6 \cdot 10^{10}$
B.R.$\to(l^+l^-\pi^+\pi^-)$ / $\pi^+\pi^-$	$4 \cdot 10^{-5}$	$640 \cdot 10^3$	$2 \cdot 10^{-5}$	$320 \cdot 10^3$
Accept. 2-75 mrad + K^0_S	0.52	$333 \cdot 10^3$	0.75	$240 \cdot 10^3$
Reconstr. eff. & sel. cuts	0.81*0.7	$190 \cdot 10^3$	0.9*0.25	$54 \cdot 10^3$
Trigger efficiency	0.64	$121 \cdot 10^3$	0.85	$46 \cdot 10^3$
Tagging eff. (P_T^{lept}>1.)	0.16	$19.4 \cdot 10^3$	0.16	$7.3 \cdot 10^3$
Dilution $\langle 1/(1+x^2)\rangle^2$	$(0.75)^2$	$10.9 \cdot 10^3$	$(0.75)^2$	$4.1 \cdot 10^3$
$[(\text{good-bad})/(\text{good+bad})]^2$	$(0.75)^2$	$6.1 \cdot 10^3$	$(0.75)^2$	$2.3 \cdot 10^3$
Oscillation time fit effic.	0.32	$2.0 \cdot 10^3$	0.46	$1.1 \cdot 10^3$
ERROR ON A = sin (2Φ)		± 0.023		± 0.031

Table 4. LHB estimated CP violation sensitivities for decay channels $B^\circ \to J/\Psi + K^0_S$ and $B^\circ \to \pi^+\pi^-$

CONCLUSIONS

Encouraging results have been obtained so far in extracting SPS protons by channeling in a bent crystal , reaching unprecedented extraction efficiencies. Provided that the bent crystal can be integrated in the LHC magnetic lattice as a 'normal' collimator, an 8 TeV extracted proton beam with an intensity of $2 \cdot 10^8$ protons/s can be obtained.

A large acceptance and powerful spectrometer has been presented offering good efficiency, small background contamination and excellent systematics control for B detection.

The capability of the proposed apparatus to trigger on B' s, reconstruct and tag their decay channels with B.R. of the order of 10^{-5} has been discussed. An absolute error of $\pm$ 2 to 3 10^{-2} on the CP violating parameter $\Lambda = \sin(2\Phi)$ can be reached, where Φ is the angle related respectively to the decay $B^\circ \rightarrow J/\Psi + K^0_S$ and to $B^\circ \rightarrow \pi^+\pi^-$ in the so called unitarity triangle.

ACKNOWLEDGEMENTS

The shaping-up and the design of the LHB apparatus in the result of the enthusiasm and ingenuity of all the colleagues of the LHB collaboration and of the related RD22 program. I'm indebted to all of them and in particular to G. Carboni for many enlightening discussions.
It is also a pleasure to thank the organizing committee for the stimulating, friendly and collaborative atmosphere they have been able to create in the Liblice workshop.

REFERENCES

[1] C.H. Sun et al., Proc. 1984 Summer Study on the Design and Utilization of the SSC, Snowmass (1984) p.483.
B. Cox et al., Proc. 1988 Summer Study on the Design and Utilization of the SSC, Snowmass 1988 (World Scientific, Singapore, 1989) p.536.

[2] Expression of Interest for a Bottom Collider Detector at SSC, SSC-EOI#8, (1990).
Internal Target Physics at the SSC, SSC-EOI#13, (1990).
An Expression of Interest in a Super Fixed Target Beauty Facility (SFT) at the Super-conducting Super Collider, SSC-EOI#14, (1990).

[3] Proceedings of the General Meeting on LHC Physics & Detectors Evian, March 1992
The following Expression of Interest were presented:
- An LHC collider Beauty experiment for CP-violation measurements
- Measurement of CP-violation in B-decays using an LHC extracted beam : the LHB Collaboration.
- A study of CP violation in B-meson decays using a gas jet at LHC

[4] G. Carboni. LHB's or Large Hadron Beauty Factories.
Proceedings "Les Rencontres de Physique de la Vallee d'Aoste" La Thuile 1991.

[5] See for instance: "Physics Rationale for a B Factory" CLNS 91-1043

[6] M. Lusignoli, L. Maiani, G. Martinelli, L. Reina
"Mixing and CP-violation in K and B Mesons: a lattice QCD point of view" N.P. B369(1992)139.

[7] Design Study of LHC. CERN 91--03

[8] V.V. Avdeichikov et al. JINR 1-84 (also in FNAL FN-429 (1986))
M. Bavizhev et al. Proc. 1989 UNK Workshop.

[9] "A proposal to test beam extraction by crystal channeling at the SPS: a first step towards a LHC extracted beam". CERN/DRDC 91-25

[10] Status Report on RD22 by S. Weisz: “Crystal Extraction at the SPS “. CERN/DRDC 92-51

[11] E. Uggerhoj Private communication.

[12] A more detailed analysis description of H8 data is being prepared for pubblication.

[13] W. Scandale in : Proceedings of the LHC Workshop (G. Jarlskog and D. Rein Editors,Aachen 1990), Vol. III p. 760 .

[14] K. Potter Private communication.

[15] S.I. Baker in : Relativistic Channeling, eds R.A. Carrigan, Jr and J.A. Ellison (Plenum, New York, 1987) p.391 .

[16] K. Elsener Private communication.

[17] LOI "An Experiment to study CP violation in the B system using an internal target at the HERA proton ring" DESY-PRC 92/04 Oct. 92.

[18] See for instance the Status Report presented at CERN SPSLC on 19/1/93 by L. Rossi.

[19] Aghinolfi et al. CERN/ECP 91-25

[20] J. Seguinot and T. Ypsilantis " Ring imaging Cherenkov counters". CERN-LAA/PI/91-004

[21] D. Autiero et al. ' Characteristics and performances of an electromagnetic shower sampling calorimeter with wavelength shifting fibre readout'. To be submitted to NIM.

[22] F. Ferroni et al. The LHB muon trigger scheme. Contribution to this conference.

[23] G. Darbo, L. Rossi NIM A289 (1990) 584

[24] T. Sjostrand, PYTHIA Version 5.5, CERN-TH 6488/92 (1992)

[25] F. Costantini LHB Internal note 13/2/92.

[26] C. Kourkoumelis et al. P.L. 91B (1980) 481

[27] R. Waldi Internal note LHB 92-02

[28] R. Waldi LHB Note 92-01 . All the evaluations here just recalled, are fully developed in this note.

[29] G. Carboni. "A few comments on asymmetry measurements". LHB internal note 28/8/91.

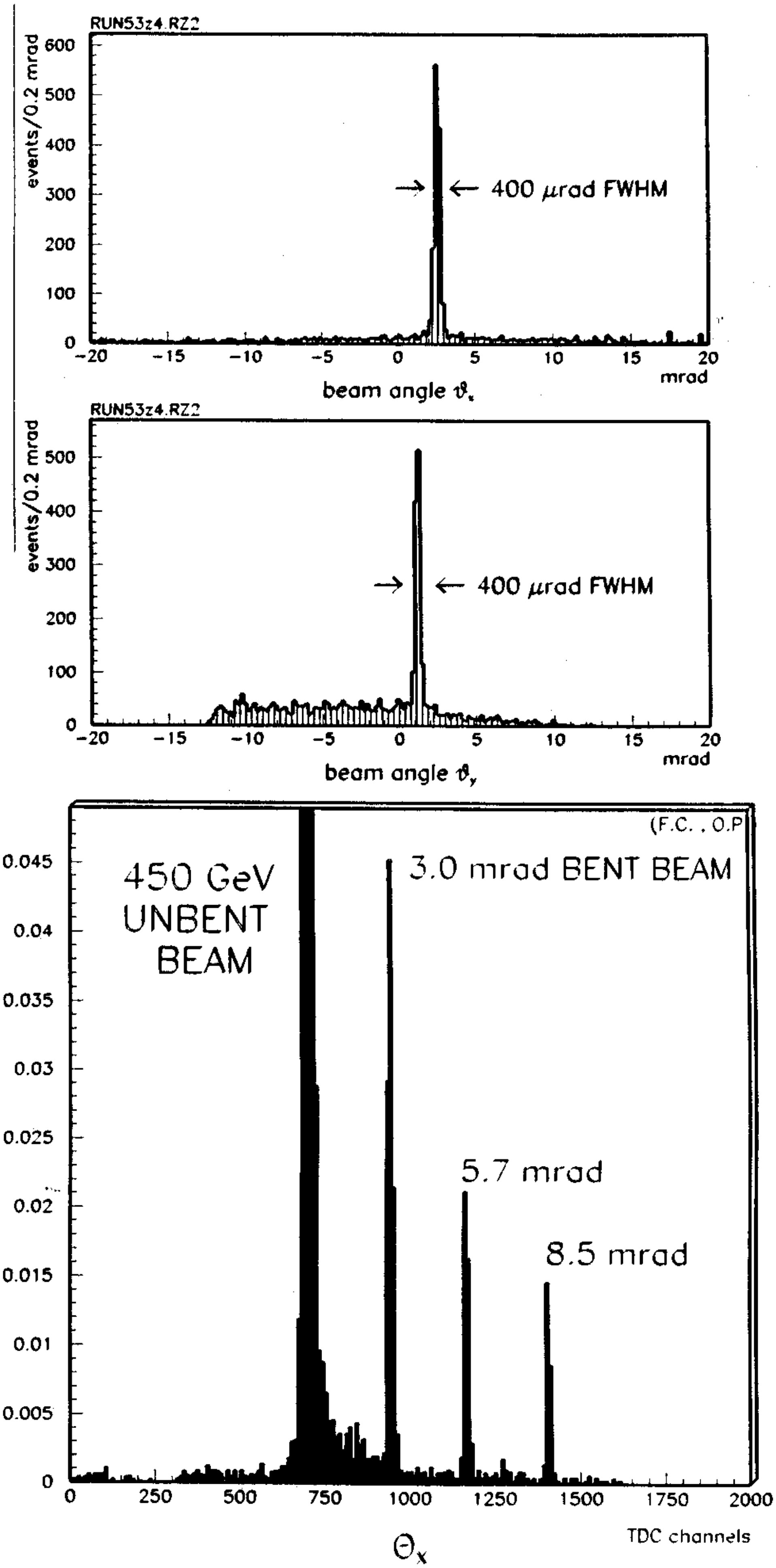

FIGURE 1. 1a) Horizontal and vertical divergence of the extracted beam as measured by the MSGC. 1b) Overlapped and normalized distributions of the 450 GeV/c proton beam bent by crystal channeling at three different bending angles.

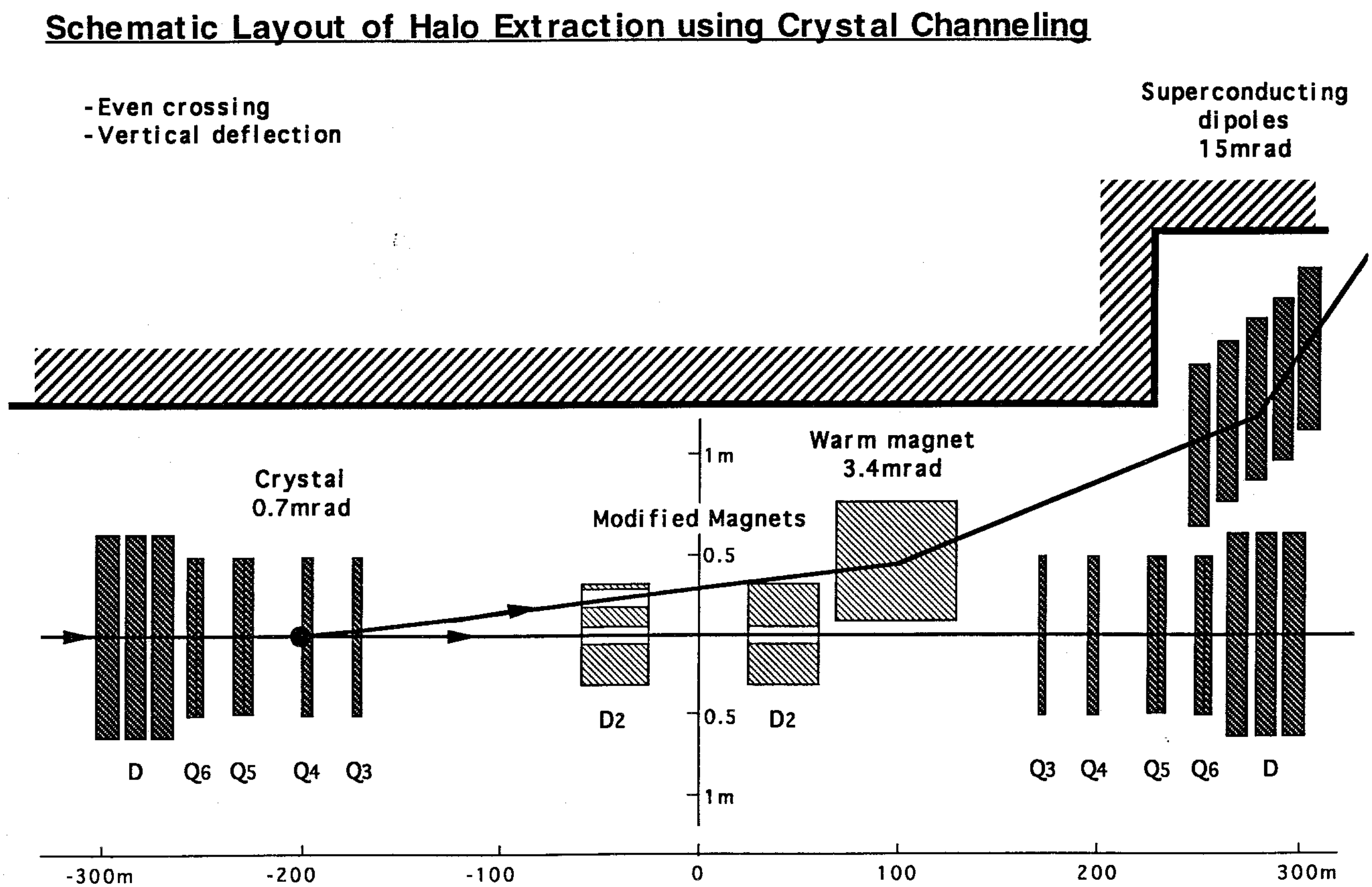

FIGURE 2. Shematic layout of vertical halo extraction using channeling in a bent silicon crystal. After the warm septum magnet the extracted beam is bent by a string of five superconducting dipoles of the LHC type [14].

LHB DETECTOR

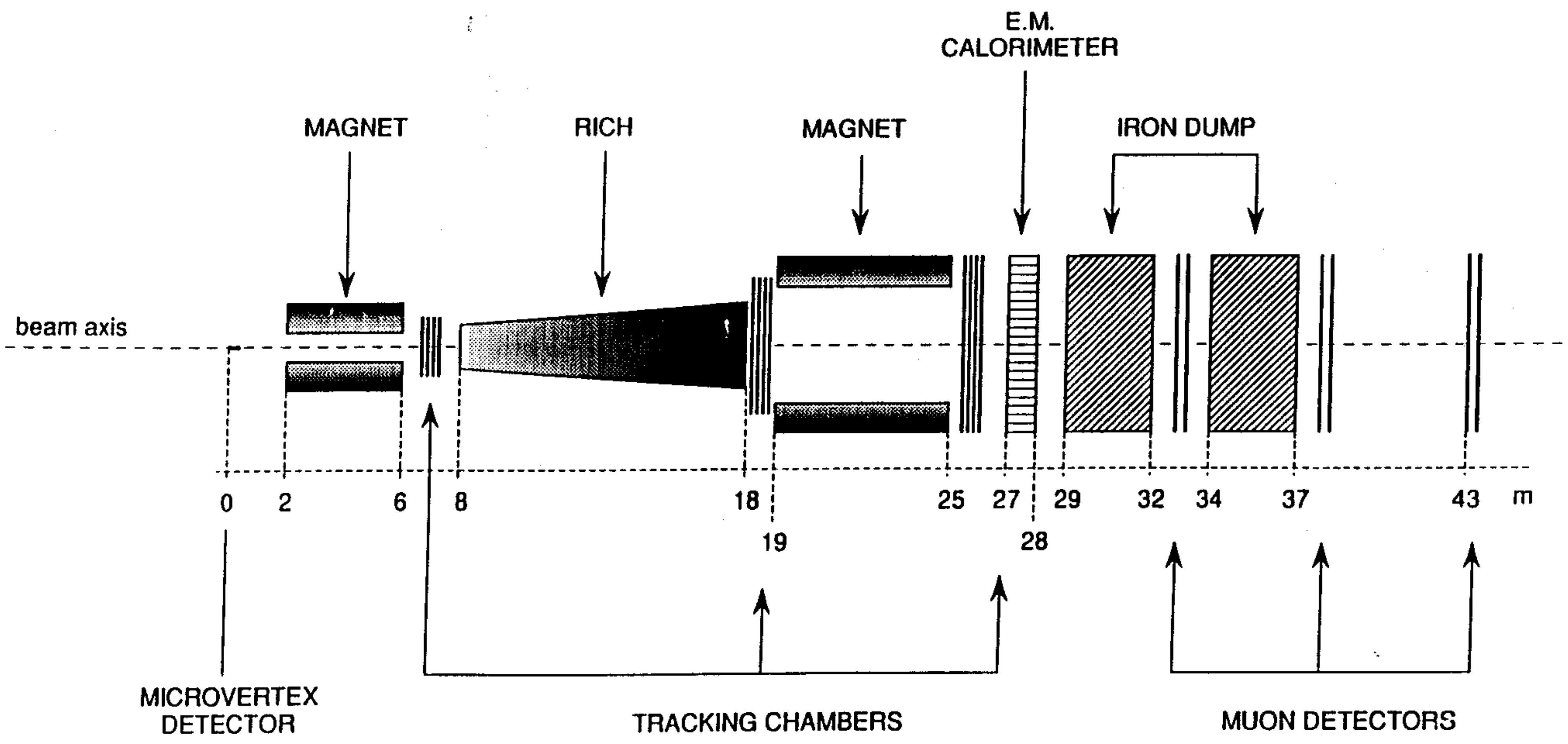

FIGURE 3. The LHB spectrometer. The two dipoles have the same bending power but opposite B field .

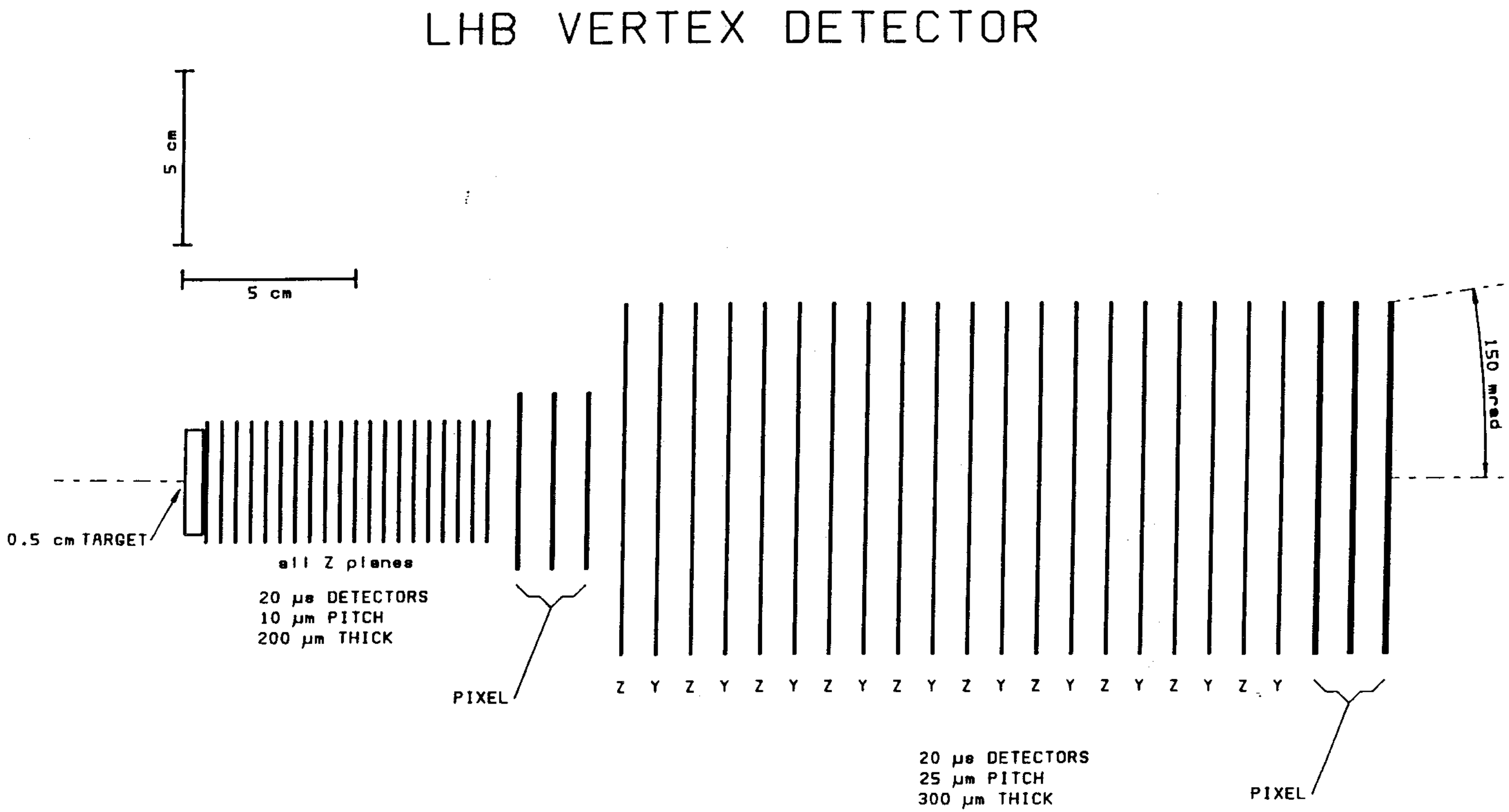

FIGURE 4. The LHB micro-vertex detector. The decay (first section) and the vertex (second section) detectors are made of micro-strips planes. The vertex detector is sandwiched by three pixel planes.

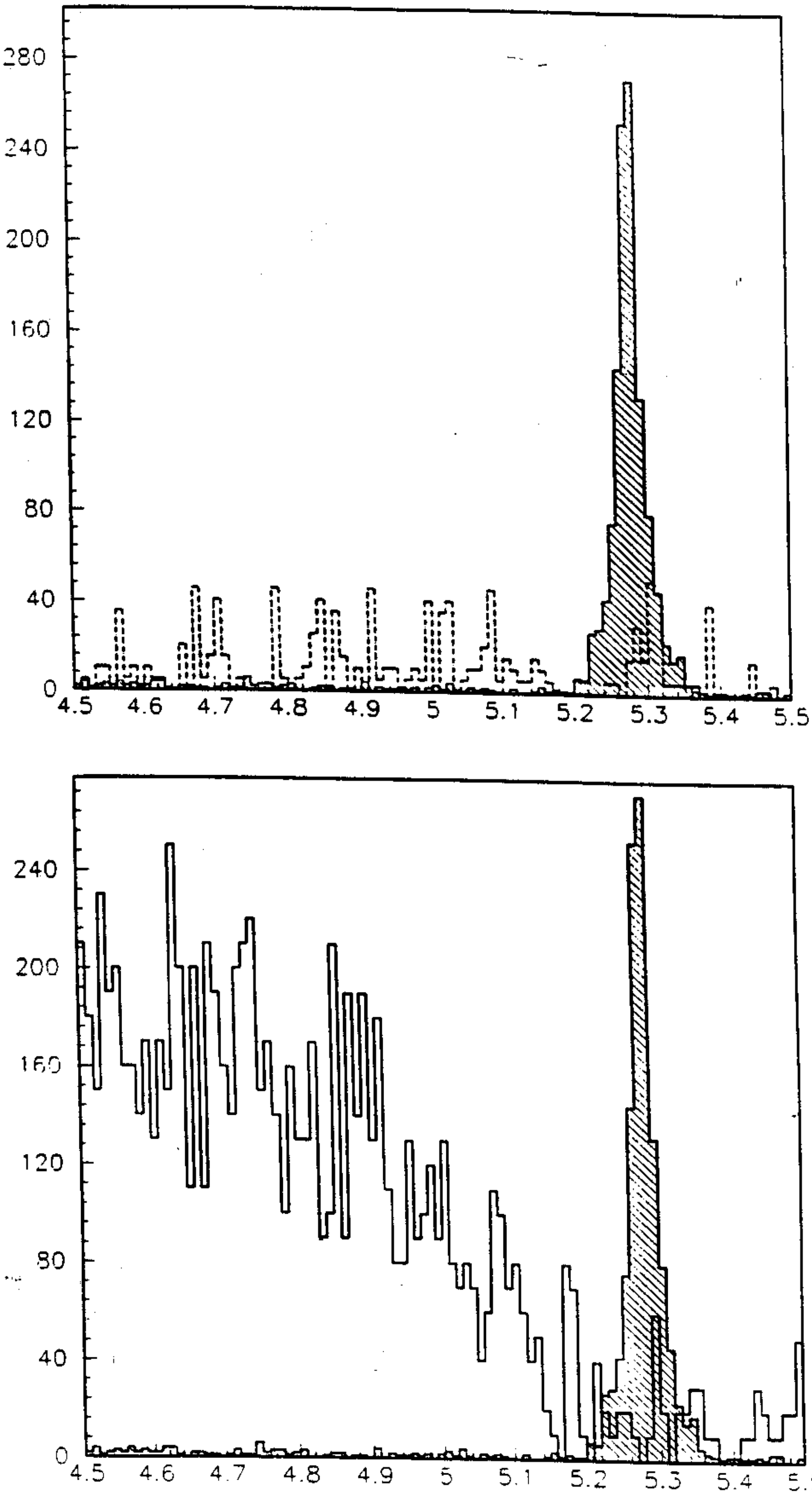

FIGURE 5. Invariant mass distribution for the decay $B^\circ \rightarrow J/\Psi + K^0_S \rightarrow \mu^+\mu^- + \pi^+\pi^-$ (see text for assumed B.R.'s and applied cuts). The B° invariant mass is obtained by a mass constrained fit of J/Ψ and K°. 5a) The non resonant combinatorial background due to "strong" J/Ψ production $+ K^\circ$ and to inclusive $B^\circ \rightarrow J/\Psi + X + K^\circ$ is shown. 5b) The contamination of the decay channel $B^\circ \rightarrow J/\Psi + K^0_S + \pi^0$ is shown assuming a 10 times bigger branching ratio.

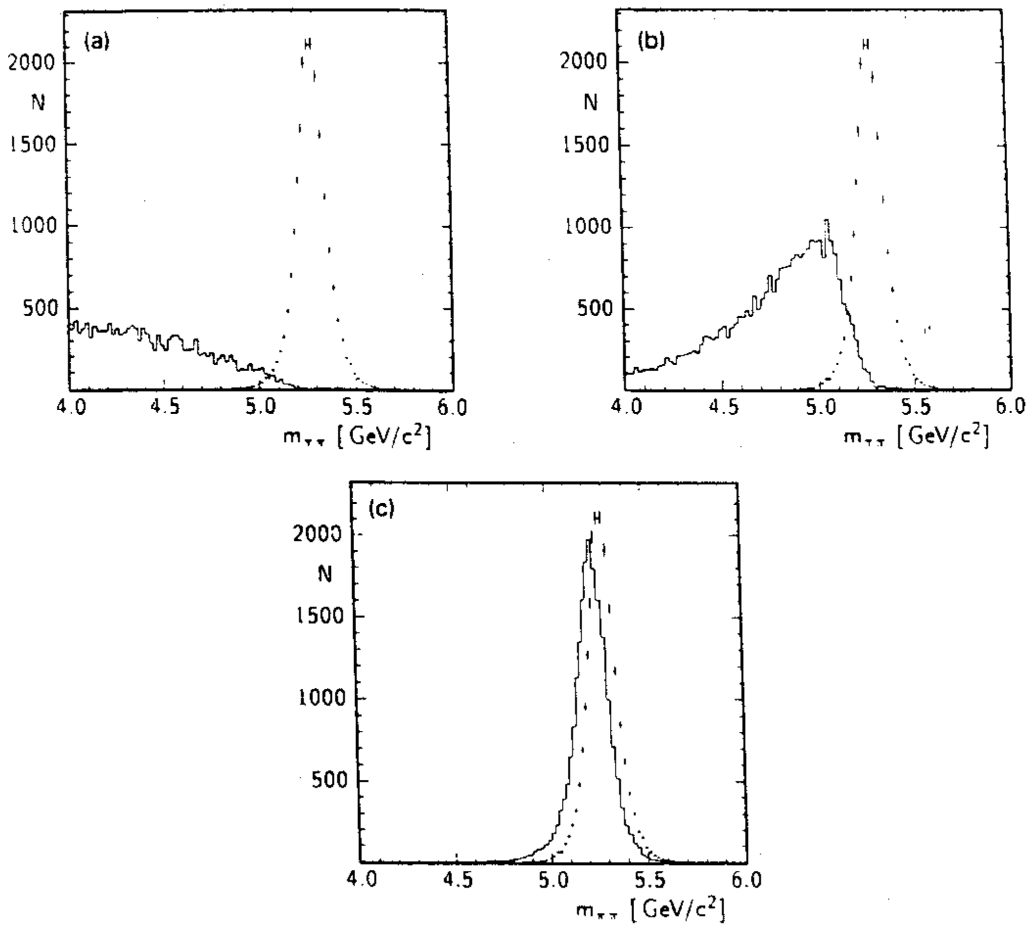

FIGURE 6. Invariant mass distribution for the decay $B^\circ \to \pi^+\pi^-$ (crosses) and 6a) a four times larger number of non resonant $B^\circ \to \pi^+\pi^-\pi^0$ 6b) a four times larger number of $B^\circ \to \rho^\pm\pi^\pm$ 6b) the same number of misidentified $B^\circ \to K^+\pi^-$.

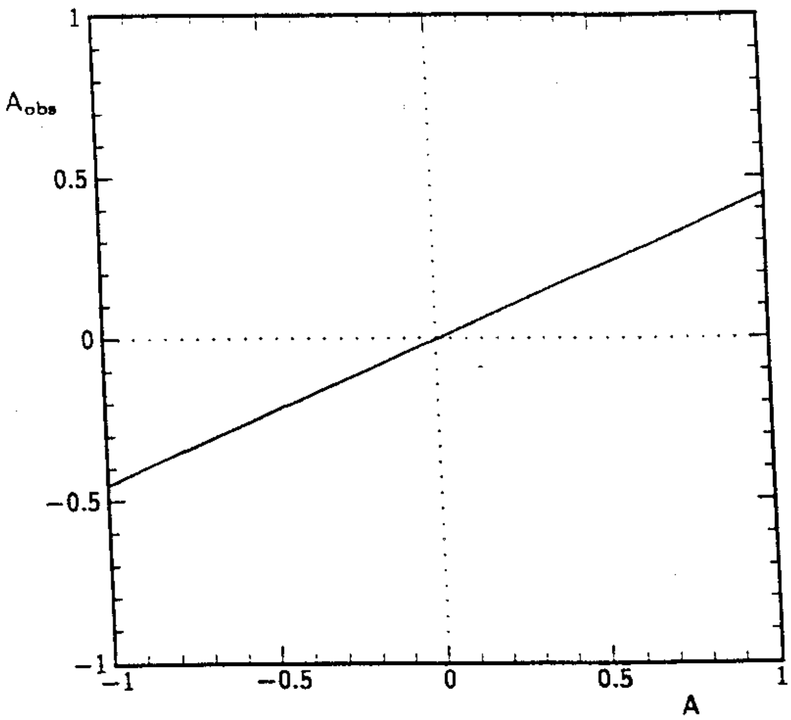

FIGURE 7. Observed asymmetry $A_{obs} = I + K \cdot A$ where A is the physical asymmetry, I is the "intrinsic" global asymmetry and K is a "dilution factor". In the linear approximation and with the choice of cuts and parameters mentioned in the text I = -0.003 and K = 0.45 is obtained.